A path-integral–Riemann-space approach to the electromagnetic wedge diffraction problem

Richard W. Ziolkowski
Electronics Engineering Department, Lawrence Livermore National Laboratory, P. O. Box 808, L-156, Livermore, California 94550

(Received 24 October 1984; accepted for publication 30 April 1986)

A path integral constructed over a particular Riemann space is developed and applied to two-dimensional wedge problems. This path-integral–Riemann-space (PIRS) approach recovers the exact solutions of the heat conduction and the corresponding electromagnetic wedge problems. A high-frequency asymptotic evaluation of the PIRS electromagnetic wedge solution returns the standard geometrical theory of diffraction (GTD) results. Ramifications of this approach and its relationships with known path-integral methods are examined.

I. INTRODUCTION

Many quantum mechanical applications of path integrals defined on multiconnected spaces have appeared in the literature.[1–5] Similarly, using a double-sheeted Riemann surface Buslaev[6] established the viability of the path-integral approach to the scattering of electromagnetic waves from smooth conductors. However, in spite of the known importance of the multiconnected space description of diffraction phenomena (see Sommerfeld[7] or Carslaw[8]), the application of an analogous path-integral approach to electromagnetic diffraction problems has been neglected. It is the object of this paper to demonstrate the utility of a path-integral–Riemann-space approach in wedge diffraction problems and to point out several interesting aspects of the resultant representations of the solutions.

In Secs. II–V, a path-integral–Riemann-space (PIRS) approach is developed and applied to the electromagnetic diffracting (perfectly conducting) wedge problem. As in Buslaev[6] and Lee,[9] the diffraction problem is first transformed to its equivalent heat conduction problem. The latter is treated with the PIRS approach. The transform of the resultant expression returns the exact wedge diffraction solution. A high-frequency asymptotic approximation of the PIRS solution is given in Sec. VI. It recovers the results given by Keller's geometrical theory of diffraction (GTD).[10] In Sec. VII, several properties of the PIRS solution to the electromagnetic and heat conduction wedge problems are described. Relations based upon the multivaluedness of the solutions are derived that demonstrate that the modification of free-space by the wedge leads to the diffraction effects. Moreover, it is shown that the half-plane propagator satisfies a transition condition that is characteristic of the underlying Riemann space and is associated with a particular Riemann–Hilbert problem.[11] The relationships of the PIRS approach with analogous quantum mechanical methods are also discussed. For instance, the connection between the PIRS method and the constrained path-integral approach[12–16] is established. It indicates that a PIRS wedge analysis may prove useful for studies of fractional charge quantization. Other salient features of the PIRS approach suggest its applicability to related problems of interest involving entangled polymers in molecular biology, Ising models in statistical mechanics, and soliton and instanton models in quantum field theory.

II. WEDGE DIFFRACTION PROBLEM

A. Problem configuration

Consider in two dimensions the diffraction of the field due to a unit point source by a perfectly conducting wedge with exterior angle $\beta\pi$, $1<\beta<2$. The electric field vector is assumed to be parallel to the edge of the wedge (E-polarized field). This is equivalent to the three-dimensional diffraction problem in which a line source is parallel to the edge of a wedge of infinite extent. The scattered field is also E-polarized and is assumed to satisfy the radiation condition at infinity.

A polar coordinate system is erected whose origin is located at the edge of the wedge. Angles measured in a counterclockwise direction from the upper edge of the wedge defined to be $\theta = 0$ are positive. The lower edge is defined by $\theta = \beta\pi$. The physical space $[0, \infty[\times [0, \beta\pi]$, exterior to the wedge, is denoted by P. The observation point is located at $\mathbf{r} = (r,\theta)$; the unit source $\delta(\mathbf{r}-\mathbf{r}_0)$ is located at $\mathbf{r}_0 = (r_0,\theta_0)$. This geometry is shown in Fig. 1.

B. The Riemann spaces P_2 and P_∞

The original diffraction problem in the physical space P is simplified by considering diffraction in a space P_2 con-

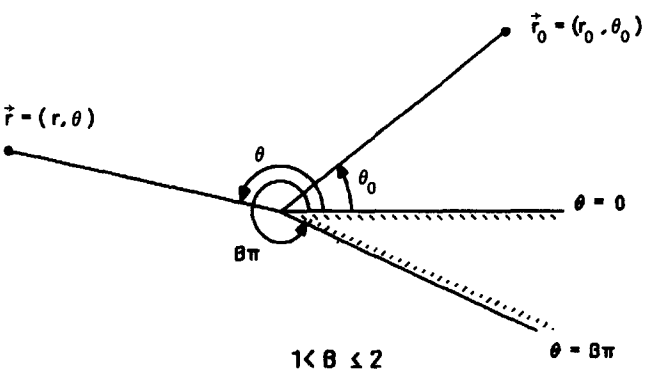

FIG. 1. Geometry of the two-dimensional diffraction by a wedge problem.

 0022-2488/86/092271-11$02.50

structed as follows. Take two replicas of P, say P_+ and P_-, and join them along the boundary Σ of the wedge. Then $P_2 = P_+ \cup P_- \cup \Sigma$. The spaces P_+ and P_- will be called, respectively, the upper and lower sheets of P_2; the space P_+ is identified with the physical space P. To suggest pictorally the two sheets, the "edge" of P_- is drawn outside of that of P_+ as illustrated in Fig. 2(a). A function $U(\mathbf{r})$ over P_2 will be a wave function if it satisfies the Helmholtz equation

$$\{\Delta + k^2\}U(\mathbf{r}) = 0 \tag{2.1}$$

over P_+ and P_- (open sets) and if the limiting values U_+ and U_- of $U(\mathbf{r})$, when $\mathbf{r}$ approaches Σ from P_+ and P_-, are opposite and if the corresponding normal derivatives on Σ toward P_+ and P_- are continuous:

$$\text{boundary conditions} \begin{cases} U_+ + U_- = 0, \\ \partial_n U_+ = \partial_n U_-, \end{cases} \text{ on } \Sigma . \tag{2.2}$$

The space P_2 is a Riemann surface, and its use here is very similar to the device introduced by Sommerfeld[7] for the half-plane problem and by Buslaev[6] for the convex body case. Natural coordinates in P_2 are the distance r to the origin and the polar angle θ counted from the upper edge of the wedge. This angle varies from 0 to $\Omega = 2\pi\beta$ and the angle

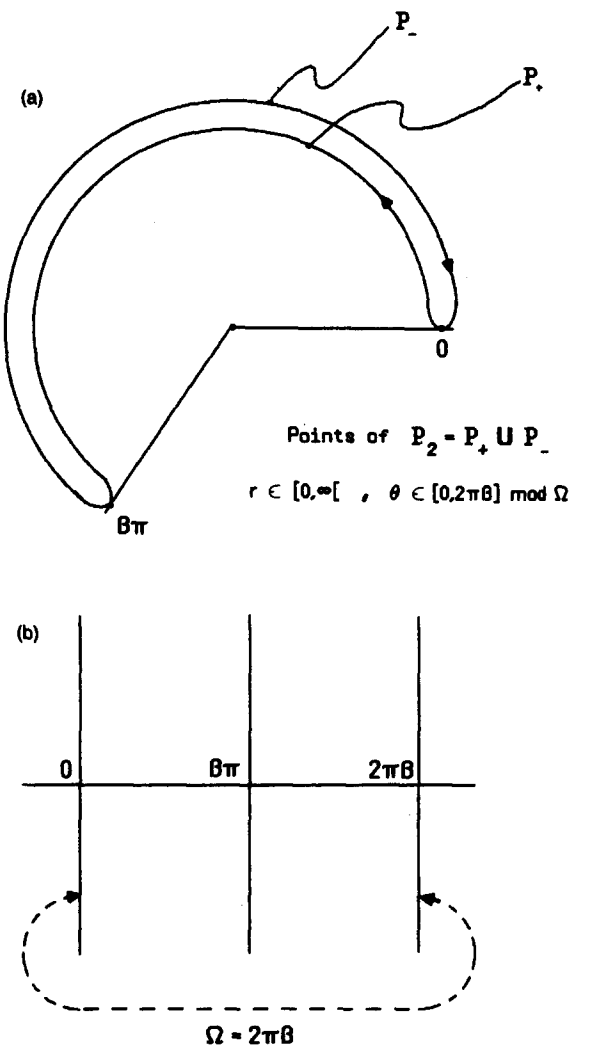

FIG. 2. Representations of the space P_2: (a) as a two-sheeted Riemann surface and (b) as its angular extent.

$\theta = 2\pi\beta$ is identified with $\theta = 0$. This geometry is shown in Fig. 2(b).

Note that the angles $\theta = 0, \beta\pi$ have no special properties. In fact, the effect of introducing P_2 may be considered as "erasing" the boundaries of the wedge. The boundary conditions are satisfied by locating an image source on P_2 (specifically, on the lower sheet P_-) at $\mathbf{r}_0' = (r_0, -\theta_0)$. The desired field can then be decomposed as

$$U(\mathbf{r}) = K(\mathbf{r},\mathbf{r}_0) - K(\mathbf{r},\mathbf{r}_0') , \tag{2.3}$$

where, for example, $K(\mathbf{r},\mathbf{r}_0)$ represents the field at $\mathbf{r}$ due to the source point at $\mathbf{r}_0$. Since reciprocity must be satisfied, $K(\mathbf{r},\mathbf{r}_0')$ must be of the same form as $K(\mathbf{r},\mathbf{r}_0)$; the former is obtained from the latter by a simple substitution $\theta_0 \to -\theta_0$. Hence, it will only be necessary to consider the function $K(\mathbf{r},\mathbf{r}_0)$.

The solution of the H-polarized problem (the magnetic field vector parallel to the edge of the wedge) is simply (2.3) with a plus sign instead of the minus sign:

$$U(\mathbf{r}) = K(\mathbf{r},\mathbf{r}_0) + K(\mathbf{r},\mathbf{r}_0') . \tag{2.3'}$$

It satisfies the P_2 boundary conditions

$$\text{boundary conditions} \begin{cases} U_+ = U_-, \\ \partial_n U_+ + \partial_n U_- = 0, \end{cases} \text{ on } \Sigma . \tag{2.2'}$$

Thus, it will not be necessary to consider that case explicitly.

The space P_∞ is constructed from an infinite number of copies of P_2. It is the covering space of P_2. The polar angle θ in P_∞ is any real number instead of being modulo 2π. Thus, for any point $\mathbf{r} = (r,\theta)$ in P_2, there are an infinite number of points (preimages) in P_∞: $(r,\theta + m\Omega)$, $m = 0, \pm 1, \pm 2, \ldots$, whose projections from P_∞ onto P_2 coincide with $\mathbf{r}$.

The desired solution in P_2, $K(\mathbf{r},\mathbf{r}_0)$, is obtained from the corresponding solution in P_∞, $K_\infty(r,\theta;r_0,\theta_0)$, by "folding" it onto P_2; i.e., by summing the fields at all of the preimages:

$$K(\mathbf{r},\mathbf{r}_0) = \sum_{m=-\infty}^{\infty} K_\infty(r,\theta + m\Omega;r_0,\theta_0) . \tag{2.4}$$

One can interpret the image contributions as multiply reflected waves between the boundaries 0 and Ω of P_2. The problem on P_∞ corresponds to one involving a perfectly absorbing wedge. This construction was used in a similar context by Deschamps[17] and by Felsen and Marcuvitz[18] and for quantum mechanical problems by Schulman.[3–5]

III. PATH-INTEGRAL SOLUTION OF A HEAT CONDUCTION EQUATION

The path integral solution of the heat conduction equation

$$\{\partial_\tau - \Delta\}G_F(x,x_0;\tau) = 0 , \tag{3.1}$$

which reduces to $\delta(x - x_0)$ for $\tau = 0$, is reviewed briefly to establish notations. The points x_0 and x are assumed to be in an n-dimensional space $X \equiv \mathbb{R}^n$.

Let γ be a path; i.e., a parametrized arc of a curve in X. It is a map of a segment $[\alpha,\beta]$ of the real axis $\mathbb{R}$ into X and is assumed at least to be continuous. The end points are taken to be $x_0 = \gamma(\alpha)$ and $x = \gamma(\beta)$. Thus,

$$\gamma: [\alpha,\beta] \subset \mathbb{R} \to X: \ \tau \to \gamma(\tau): \ (\alpha,\beta) \mapsto (x_0,x) .$$

Let Γ be the set of continuous paths γ joining x_0 to x in time τ.

The path integral solution of (3.1) is[19]

$$G_F(x,x_0;\tau) = \int_\Gamma F(\gamma)\,\mathscr{D}\gamma\,. \tag{3.2}$$

The "value" $F(\gamma)$ assigned to a path $\gamma\in\Gamma$ is taken to be the probability of going from x_0 to x in time τ following the path γ: $F(\gamma)=\exp[-E(\gamma)]$, where the energy of a particle of mass $\frac{1}{2}$ along γ is $E(\gamma)=\frac{1}{2}\int_0^\tau \dot\gamma^2\,d\tau$, $\dot\gamma = d\gamma/d\tau$ being the velocity of that particle along γ. The quantity $\mathscr{D}\gamma$ is difficult to establish; it represents the measure of the path space. The standard method of giving a meaning to (3.2) is heuristic; the scheme imitates the process that leads to a Riemann integral.

Let each γ be represented by a skeleton γ_s constructed from the $(N+1)$ points $(x_0,x_1,\ldots,x_N=x)$ in the image of γ such that

$$\gamma_s:\ (\tau_0=\alpha,\tau_1,\tau_2,\ldots,\tau_N=\beta)\mapsto(x_0,x_1,x_2,\ldots,x_N=x)\,.$$

A broken path γ_N can be constructed from these points by associating to each consecutive pair (τ_{j-1},τ_j) mapped into (x_{j-1},x_j) a path segment $\delta_j\gamma$, chosen in a prescribed manner. A standard choice is to make the image of $[\tau_{j-1},\tau_j]$ by $\delta_j\gamma$ into a straight segment described uniformly in τ; i.e.,

$$\delta_j\gamma:\ [\tau_{j-1},\tau_j]\to X:\ \tau\mapsto x_j=\frac{\delta_j x}{\delta_j\tau}(\tau-\tau_{j-1})+x_{j-1}\,.$$

The notation $\delta_j(\cdot)$ designates increments of $(\cdot)$ corresponding to the jth step (or jth segment); e.g., $\delta_j\tau=\tau_j-\tau_{j-1}$. Other choices are possible.

The heuristic definition of the path integral (3.2) is based on approximating each γ by some γ_N; hence, Γ by Γ_N, the set of broken (discrete) paths γ_N. The preceding construction of the set of broken paths Γ_N, which will be referred to as *discretization*, depends on $n(N+1)$ real parameters, provided that the τ_j's are chosen in a systematic manner. For instance, let $\tau_j=\alpha+j\Delta\tau$, where $\Delta\tau=(\beta-\alpha)/N$. One then has the correspondence

$$\gamma_N\leftrightarrow(x_0,x_1,\ldots,x_N)\in\mathbb{R}^{n(N+1)}\,.$$

Thus, with the fixed end points x_0 and $x_N=x$, the Euclidean measure in $\mathbb{R}^{n(N-1)}$ can be used to define $\mathscr{D}\gamma_N$. In the limit as $N\to\infty$ and $\max\delta_j\tau\to0$, The definition of the path integral (3.2) becomes

$$\int_\Gamma F(\gamma)\,\mathscr{D}\gamma=\lim_{N\to\infty}\int_{\Gamma_N}F(\gamma_N)\,\mathscr{D}\gamma_N\,. \tag{3.3}$$

The value $F(\gamma_N)$ assigned to the discretized path γ_N is the product $F(\gamma_N)=\prod_{j=1}^N F(\delta_j\gamma)$ of functions defined for each of the steps $\delta_j\gamma$ used to construct γ_N. Those functions represent the probability that the particle at x_{j-1} moves to x_j in the time interval from τ_{j-1} to τ_j and are defined as $F(\delta_j\gamma)=\Phi_{2\delta_j\tau}(\delta_j x)$, where

$$\Phi_\sigma(\xi)=(2\pi\sigma)^{-n/2}\exp(-|\xi|^2/2\sigma)\,.$$

Thus, with the coefficient $A_N=\prod_{j=1}^N(4\pi\delta_j\tau)^{-n/2}$ and the energy

$$\mathrm{E}(\gamma_N)=\sum_{j=1}^N E(\delta_j\gamma)\equiv\sum_{j=1}^N\frac{(\delta_j x)^2}{4\delta_j\tau}\,,$$

the discretization of the path integral (3.2) becomes

$$G_F(x,x_0;\tau)=\lim_{N\to\infty}A_N\int_{\Gamma_N}\exp[-E(\gamma_N)]\,\mathscr{D}\gamma_N\equiv\lim_{N\to\infty}\left(\frac{4\pi\tau}{N}\right)^{-nN/2}\int_{-\infty}^{\infty}\cdots\int\exp\left[-\sum_{j=1}^N E(\delta_j\gamma)\right]dx_1\,dx_2\cdots dx_{N-1}\,. \tag{3.4}$$

Now consider the polar coordinate form of the path-integral expression (3.4) when $n=2$. In $\mathbb{R}^2$, the squared distance between the two points $\mathbf{r}_j=(r_j,\theta_j)$ and $\mathbf{r}_{j-1}=(r_{j-1},\theta_{j-1})$ is

$$|\delta_j\mathbf{r}|^2=r_j^2+r_{j-1}^2-2r_jr_{j-1}\cos(\theta_j-\theta_{j-1})$$

and the measure

$$dx_1\cdots dx_{N-1}=\prod_{j=1}^{N-1}r_j\,dr_j\,d\theta_j\,.$$

Thus, with $\epsilon=\tau/N$ the expression (3.4) when $n=2$ can be represented in $\mathbb{R}^2$ as

$$G_F(\mathbf{r},\mathbf{r}_0;\tau)=\lim_{N\to\infty}(4\pi\epsilon)^{-N}\int_{\mathbb{R}^2}\cdots\int\exp\left[-\sum_{j=1}^N\frac{r_j^2+r_{j-1}^2}{4\epsilon}\right]\exp\left[\sum_{j=1}^N\left(\frac{r_jr_{j-1}}{2\epsilon}\right)\cos(\theta_j-\theta_{j-1})\right]\prod_{j=1}^{N-1}r_j\,dr_j\,d\theta_j\,. \tag{3.5}$$

As shown in Ref. 20, the exact (free-space) solution

$$G_F(\mathbf{r},\mathbf{r}_0;\tau)=(4\pi\tau)^{-1}\exp[-(r^2+r_0^2)/4\tau]\exp[(rr_0/2\tau)\cos(\theta-\theta_0)]\equiv(4\pi\tau)^{-1}\exp[-|\mathbf{r}-\mathbf{r}_0|^2/4\tau] \tag{3.6}$$

is generated from Eq. (3.5). This result will be duplicated from the PIRS point of view in Sect. VII.

IV. PATH-INTEGRAL SOLUTIONS ON P_∞

Returning now to the wedge problem, the propagator $K_\infty(\mathbf{r},\mathbf{r}_0)$, which satisfies on P_∞ the equation

$$\{\Delta+k^2\}K_\infty(\mathbf{r},\mathbf{r}_0)=-\delta(\mathbf{r}-\mathbf{r}_0)\,, \tag{4.1}$$

is desired. It can be generated by considering the corresponding parabolic equation problem; i.e., the solution $G_\infty(\mathbf{r},\mathbf{r}_0;\tau)$ of the heat conduction equation

$$\{\partial_\tau-\Delta\}G_\infty(\mathbf{r},\mathbf{r}_0;\tau)=0\,, \tag{4.2}$$

which satisfies the initial condition

$$\lim_{\tau\to0}G_\infty(\mathbf{r},\mathbf{r}_0;\tau)=\delta(\mathbf{r}-\mathbf{r}_0)\,, \tag{4.3}$$

is related to the solution of (4.1) as

$$K_\infty(\mathbf{r},\mathbf{r}_0)=\int_C d\tau\, e^{k^2\tau}G_\infty(\mathbf{r},\mathbf{r}_0;\tau)\,, \tag{4.4}$$

where C is a contour in the complex plane from $\tau=0$ to infinity. The choice of the contour is independent of k (see Ref. 6).

Following the scheme outlined in the previous section, the path-integral representation of the P_∞ propagator G_∞ is constructed. It is identical to the (free-space) expression (3.5) except that the integrations must now be realized over P_∞-spaces rather than over $\mathbb{R}^2$-spaces. The differences lies in the integration over the angle variables. In the present case, each angle integration must be taken over the infinite inteval $]-\infty,\infty[$ rather than over the finite interval $[0,2\pi]$ used in the free-space example. The resultant P_∞ expression suggests that for its evaluation it would be advantageous to introduce a Fourier transform.

The rotational symmetry of the problem implies that G_∞ will depend only on the angle difference $(\theta-\theta_0)$:

$$G_\infty(\mathbf{r},\mathbf{r}_0;\tau)=G_\infty(r,r_0,\theta-\theta_0;\tau)\,. \tag{4.5}$$

Therefore, the Fourier transform of G_∞ is defined as

$$\begin{aligned}\hat{G}_\lambda(r,r_0;\tau)&=\frac{1}{2\pi}\int_{-\infty}^{\infty}d(\theta-\theta_0)e^{-i\lambda(\theta-\theta_0)}G_\infty(r,r_0,\theta-\theta_0;\tau)\\&=\frac{1}{2\pi}\int_{-\infty}^{\infty}d\theta\, e^{-i\lambda(\theta-\theta_0)}G_\infty(r,r_0;\theta-\theta_0;\tau)\,;\end{aligned} \tag{4.6}$$

its inverse is

$$\begin{aligned}G_\infty(\mathbf{r},\mathbf{r}_0;\tau)&=\int_{-\infty}^{\infty}d\lambda\, e^{i\lambda(\theta-\theta_0)}\hat{G}_\lambda(r,r_0;\tau)\\&\equiv\mathcal{F}(\theta-\theta_0;\lambda)[\hat{G}_\lambda(r,r_0;\tau)]\,.\end{aligned} \tag{4.7}$$

Thus, by considering $\hat{G}_\lambda$ instead of G_∞ directly, one can concentrate on the radial dependence of the propagator. Substituting the pertinent, modified version of Eq. (3.5) into Eq. (4.6) and decomposing the difference $(\theta-\theta_0)$ into

$$\begin{aligned}\theta-\theta_0&=(\theta_N-\theta_{N-1})+(\theta_{N-1}-\theta_{N-2})\\&\quad+\cdots+(\theta_1-\theta_0)\\&=\sum_{j=1}^{N}(\theta_j-\theta_{j-1})\end{aligned}$$

yields

$$\begin{aligned}\hat{G}_\lambda(r,r_0;\tau)&=\lim_{N\to\infty}\frac{1}{2\pi}\int_0^\infty\cdots\int\prod_{j=1}^{N-1}r_j\,dr_j(4\pi\epsilon)^{-N}\\&\quad\times\exp\left[-\sum_{j=1}^{N}\frac{r_j^2+r_{j-1}^2}{4\epsilon}\right]\int_{-\infty}^{\infty}\cdots\int\prod_{j=1}^{N}\left\{d\theta_j\right.\\&\quad\left.\times\exp\left[\frac{r_jr_{j-1}}{2\epsilon}\cos(\theta_j-\theta_{j-1})-i\lambda(\theta_j-\theta_{j-1})\right]\right\}.\end{aligned} \tag{4.8}$$

Note that the additional angle integration with respect to $\theta_N=\theta$ results from the integral in Eq. (4.6). Taking into account the finiteness of the propagator as $r\to0$, the expression (4.8) gives

$$\begin{aligned}\hat{G}_\lambda(r,r_0;\tau)&=(4\pi\tau)^{-1}\exp[-(r^2+r_0^2)/4\tau]I_{|\lambda|}(rr_0/2\tau)\,.\end{aligned} \tag{4.9}$$

The steps leading from Eq. (4.8) to Eq. (4.9) are described in detail in the Appendix.

Inserting the "radial" propagator (4.9) into Eq. (4.7), one obtains the representation

$$\begin{aligned}G_\infty(\mathbf{r},\mathbf{r}_0;\tau)&=(4\pi\tau)^{-1}\exp[-(r^2+r_0^2)/4\tau]\\&\quad\times\int_{-\infty}^{\infty}d\lambda\, e^{i\lambda(\theta-\theta_0)}I_{|\lambda|}\left(\frac{rr_0}{2\tau}\right),\end{aligned} \tag{4.10}$$

for the solution of the heat equation (4.2) on P_∞. Consequently, with Eq. (4.4) the desired solution of Eq. (4.1) on P_∞ is

$$\begin{aligned}K_\infty(\mathbf{r},\mathbf{r}_0)&=\int_{-\infty}^{\infty}d\lambda\, e^{i\lambda(\theta-\theta_0)}\int_C\frac{d\tau}{4\pi\tau}\\&\quad\times\exp\left[k^2\tau-\frac{(r^2+r_0^2)}{4\tau}\right]I_{|\lambda|}\left(\frac{rr_0}{2\tau}\right).\end{aligned} \tag{4.11}$$

Since (see Ref. 21, 8.424.1)

$$\begin{aligned}&\frac{1}{\pi i}\int_0^{\eta+i\infty}\exp\left[\frac{1}{2}\left(t-\frac{\xi^2+\zeta^2}{t}\right)\right]I_\nu\left(\frac{\xi\zeta}{t}\right)\frac{dt}{t}\\&\quad=J_\nu(\xi)H_\nu^{(1)}(\zeta)\,,\end{aligned}$$

where $\mathrm{Re}\,\nu>-1$, $\eta>0$, and $|\xi|<|\zeta|$, Eq. (4.11) becomes

$$K_\infty(\mathbf{r},\mathbf{r}_0)=\frac{i}{4}\int_{-\infty}^{\infty}d\lambda\, e^{i\lambda(\theta-\theta_0)}J_{|\lambda|}(kr_<)H_{|\lambda|}^{(1)}(kr_>)\,, \tag{4.12}$$

where $r_>$ is the larger of r and r_0, $r<$ the smaller. Note that expression (4.12) coincides with the *Riemann surface fundamental solution* defined by Stakgold (see Ref. 22, pp. 270–271).

V. SOLUTION OF THE WEDGE PROBLEM

As noted in Sec. II, the propagator on P_2 from the (real) source point $\mathbf{r}_0$ to the observation point $\mathbf{r}$, $K(\mathbf{r},\mathbf{r}_0)$, associated with the wedge (diffraction) problem, is generated by folding the P_∞-space solution (4.12) onto the P_2-space. The resultant expression has the form

$$\begin{aligned}K(\mathbf{r},\mathbf{r}_0)&=\frac{i}{4}\sum_{m=-\infty}^{\infty}\int_{-\infty}^{\infty}d\lambda\exp[i\lambda(\theta-\theta_0+m\Omega)]\\&\quad\times J_{|\lambda|}(kr_<)H_{|\lambda|}^{(1)}(kr_>)\,.\end{aligned} \tag{5.1}$$

However, using the Poisson summation formula,

$$\begin{aligned}\sum_{m=-\infty}^{\infty}e^{i\lambda m\Omega}&=\sum_{m=-\infty}^{\infty}e^{i2\pi m\beta\lambda}=\sum_{m=-\infty}^{\infty}\delta(\beta\lambda-m)\\&=\frac{1}{\beta}\sum_{m=-\infty}^{\infty}\delta\left(\lambda-\frac{m}{\beta}\right),\end{aligned} \tag{5.2}$$

one obtains

$$\begin{aligned}K(\mathbf{r},\mathbf{r}_0)&=\frac{i}{4\beta}\sum_{m=-\infty}^{\infty}\exp\left[i\frac{m}{\beta}(\theta-\theta_0)\right]\\&\quad\times J_{|m/\beta|}(kr_<)H_{|m/\beta|}^{(1)}(kr_>)\,.\end{aligned} \tag{5.3}$$

This expression can be immediately rewritten as

$$K(\mathbf{r},\mathbf{r}_0)=\frac{i}{4\beta}\sum_{m=0}^{\infty}\epsilon_m J_{m/\beta}(kr_<)H^{(1)}_{m/\beta}(kr_>)\times\cos\left[\frac{m}{\beta}(\theta-\theta_0)\right], \tag{5.4}$$

where the term

$$\epsilon_m=\begin{cases}1, & \text{if } m=0,\\ 2, & \text{if } m\neq 0.\end{cases}$$

Using the results of Ref. 23, it also has the integral representation

$$K(\mathbf{r},\mathbf{r}_0)=\frac{-1}{16\pi}\int_A H_0^{(1)}(kR(\alpha))\chi_\beta(\alpha,\theta-\theta_0)d\alpha, \tag{5.5}$$

where the distance $R(\alpha)=[r^2+r_0^2-2rr_0\cos\alpha]^{1/2}$ and the diffraction coefficient

$$\chi_\beta(\alpha,\psi)=\frac{2}{\beta}\frac{\sin(\alpha/\beta)}{\cos(\alpha/\beta)-\cos(\psi/\beta)}.$$

The path of integration A is shown in Fig. 3.

Consequently, with Eq. (2.3) the total solution of the wedge problem is represented as

$$\begin{aligned}U(\mathbf{r})&=K(r,\theta;r_0,\theta_0)-K(r,\theta;r_0,-\theta_0)\\&=\frac{i}{4\beta}\sum_{m=0}^{\infty}\epsilon_m\left\{\cos\left[\frac{m}{\beta}(\theta-\theta_0)\right]-\cos\left[\frac{m}{\beta}(\theta+\theta_0)\right]\right\}\\&\quad\times J_{m/\beta}(kr_<)H^{(1)}_{m/\beta}(kr_>)\\&=\frac{i}{2\beta}\sum_{m=0}^{\infty}\epsilon_m\sin\left(\frac{m\theta}{\beta}\right)\sin\left(\frac{m\theta_0}{\beta}\right)\\&\quad\times J_{m/\beta}(kr_<)H^{(1)}_{m/\beta}(kr_>)\end{aligned} \tag{5.6}$$

or as

$$U(\mathbf{r})=\frac{-1}{16\pi}\int_A H_0^{(1)}(kR(\alpha))\times[\chi_\beta(\alpha,\theta-\theta_0)-\chi_\beta(\alpha,\theta+\theta_0)]d\alpha. \tag{5.6'}$$

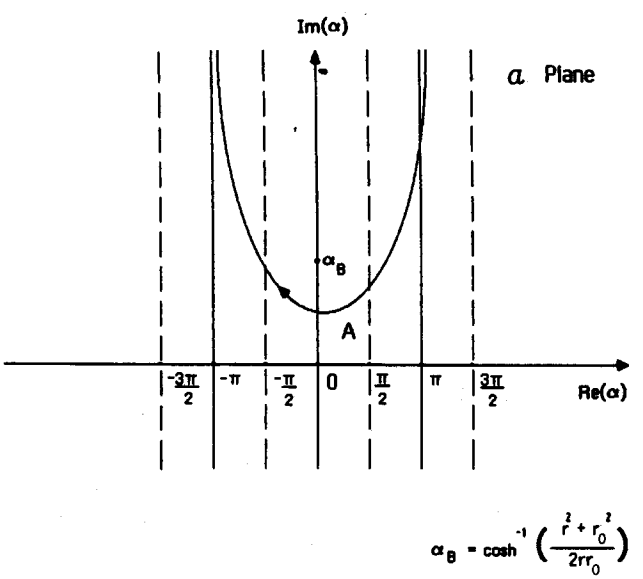

FIG. 3. Path of integration A used for the wedge solution.

These results agree with the known solutions given, for example, in Refs. 18, 21, and 24.

VI. HIGH-FREQUENCY APPROXIMATIONS OF THE WEDGE SOLUTION

The high-frequency (short-wavelength) approximation to the wedge solution (5.6) in the shadow region of the source and its image will be generated from the P_∞ solution (4.12). The GTD results given by Keller[10] are recovered. The analysis is analogous to the one used by Wu[25] to study creeping waves around a circular cylinder.

The P_∞ solution (4.12) can be rewritten as

$$K_\infty(\mathbf{r},\mathbf{r}_0)=\frac{i}{2}\int_0^\infty d\lambda\cos[\lambda(\theta-\theta_0)]\times J_\lambda(kr_<)H^{(1)}_\lambda(kr_>). \tag{6.1}$$

Asymptotically for $kx\to\infty$ the Bessel and Hankel functions $J_\lambda(kx)$ and $H^{(1)}_\lambda(kx)$ behave as

$$\begin{aligned}\lim_{kx\to\infty}J_\lambda(kx)&\sim(2/\pi kx)^{1/2}\cos\left[kx-(\lambda+\tfrac{1}{2})\pi/2\right]\\&=(2/i)[g(kx)e^{-i\lambda\pi/2}+g^*(kx)e^{i\lambda\pi/2}],\end{aligned}$$

$$\lim_{kx\to\infty}H^{(1)}_\lambda(kx)\sim(4/i)g(kx)e^{-i\lambda\pi/2},$$

where the function

$$g(kx)=(8\pi kx)^{-1/2}\exp[i(kx+\pi/4)]$$

and $g^*(kx)$ is its complex conjugate. Inserting these asymptotic forms into (6.1) and using the relation

$$\int_0^\infty d\lambda\, e^{i\lambda x}=\pi\delta(x)+\frac{i}{x},$$

one obtains the expression

$$\begin{aligned}K_\infty(\mathbf{r},\mathbf{r}_0)\sim&\,2g(kr_>)g(kr_<)[1/\psi_+-1/\psi_-]\\&-2\pi ig(kr_>)g(kr_<)[\delta(\psi_+)+\delta(\psi_-)]\\&-4\pi ig(kr_>)g^*(kr_<)\delta[(\psi_++\psi_-)/2],\end{aligned} \tag{6.2}$$

where the angles $\psi_\pm=(\theta-\theta_0)\mp\pi=\theta-(\theta_0\pm\pi)$.

In P_2 the angles $\theta=\theta_0,\theta_0\pm\pi$ correspond, respectively, to the directions of the source and the shadow boundaries of the source and its image. For a point in the shadow region of the fields incident on the wedge from the source and its image; i.e., for $\theta\epsilon]\theta_0+\pi,\Omega-(\theta_0+\pi)[$, these singular directions are not encountered. The asymptotic form of the P_∞ solution then reduces to

$$K_\infty(\mathbf{r},\mathbf{r}_0)\sim 2g(kr_>)g(kr_<)[1/\psi_+-1/\psi_-]. \tag{6.3}$$

With (2.4) and (6.3) the propagator $K(\mathbf{r},\mathbf{r}_0)$ in the shadow region has the asymptotic form

$$K(\mathbf{r},\mathbf{r}_0)\sim 2g(kr_>)g(kr_<)\times\sum_{m=-\infty}^{\infty}\left[\frac{1}{\psi_++m\Omega}-\frac{1}{\psi_-+m\Omega}\right]. \tag{6.4}$$

Since

$$\cot\xi=\frac{1}{\xi}+2\xi\sum_{m=1}^{\infty}\left[\frac{1}{\xi^2-(m\pi)^2}\right]$$

and

$$\cot\left(\frac{\phi+\psi}{2}\right)-\cot\left(\frac{\phi-\psi}{2}\right)=-2\frac{\sin\psi}{\cos\psi-\cos\phi},$$

the sum

$$\begin{aligned}2\sum_{m=-\infty}^{\infty}&\left[\frac{1}{\psi_+ + m\Omega}-\frac{1}{\psi_- + m\Omega}\right]\\&=\frac{1}{\beta}\left[\cot\left(\frac{\psi_+}{2\beta}\right)-\cot\left(\frac{\psi_-}{2\beta}\right)\right]\\&=\frac{2}{\beta}\frac{\sin(\pi/\beta)}{\cos(\pi/\beta)-\cos[(\theta-\theta_0)/\beta]}\equiv\chi_\beta(\pi,\theta-\theta_0)\end{aligned}\tag{6.5}$$

recovers the wedge diffraction coefficient and (6.4) becomes

$$K(\mathbf{r},\mathbf{r}_0)\sim g(kr_>)\chi_\beta(\pi,\theta-\theta_0)g(kr_<)\,.\tag{6.6}$$

Similarly, the image source contribution is

$$K(\mathbf{r},\mathbf{r}_0')\sim g(kr_>)\chi_\beta(\pi,\theta+\theta_0)g(kr_<)\,.\tag{6.7}$$

Consequently, with (2.3) the asymptotic form of the (E-polarized) wedge solution in the shadow region is

$$U(\mathbf{r})\sim g(kr_>)[\chi_\beta(\pi,\theta-\theta_0)-\chi_\beta(\pi,\theta+\theta_0)]g(kr_<)\,.\tag{6.8}$$

This expression coincides with Keller's GTD result. It represents the effects of the source and image fields interacting with the edge of the wedge. The presence of the additional terms in (6.2) indicates the need in the lit regions to account for the direct, geometrical optics fields in (6.8); i.e., the asymptotic forms of the source and image fields when $\mathbf{r}$ can be reached without interacting with the edge must be included in (6.8).

VII. DISCUSSION

In order to connect the present results with those in the literature, several alternate representations of the PIRS solutions will be considered. They reveal a variety of interesting properties of the PIRS approach.

The point in P_2 that lies on P_- "beneath" the point (r,θ) on P_+ is $(r,\Omega-\theta)$. The value of the P_2 wedge propagator (5.4) at that point recovers the image source contribution

$$K(r,\Omega-\theta;r_0,\theta_0)\equiv K(r,\theta;r_0,-\theta_0)\,.\tag{7.1}$$

Consequently, the wedge solutions (2.3) and (2.3′) can be represented as

$$U(\mathbf{r})=K(r,\theta;r_0,\theta_0)-pK(r,\Omega-\theta;r_0,\theta_0)\,,\tag{7.2}$$

where $p=+1$ for the E-polarized case and $p=-1$ for the H-polarized case. Their satisfaction of the P_2 boundary conditions (2.2) and (2.2′) are easily demonstrated with this expression. Moreover, since $K(r,\theta;r_0,\theta_0)$ and $K(r,\Omega-\theta;r_0\theta_0)$ represent the values of different branches of the P_2 solution at corresponding points, the E- and H-polarized wedge solutions are, respectively, simply a difference and a sum of those values.

Next, consider the sum of the values of the P_∞ solution (4.12) at the points $(r,\theta+m2\pi)$, $m=0,\pm1,\pm2,\ldots$. This sum includes at least one contribution from each P_2 surface in P_∞ and the term $K_\infty(r,\theta+m2\pi;r_0,\theta_0)$ can be viewed as the value of the mth branch of the P_∞ solution at (r,θ). As is readily shown, the free-space propagator $K_F(\mathbf{r},\mathbf{r}_0)$; i.e., the propagator in $\mathbf{R}^2$ between $\mathbf{r}_0$ and $\mathbf{r}$ with no wedge present, is recovered. In particular, with 8.531.2 of Ref. 21 and (5.2) the sum

$$\begin{aligned}\sum_{m=-\infty}^{\infty}&K_\infty(r,\theta+m2\pi;r_0,\theta_0)\\&=\frac{i}{4}\int_{-\infty}^{\infty}d\lambda\exp[i\lambda(\theta-\theta_0)]J_{|\lambda|}(kr_<)\\&\quad\times H_{|\lambda|}^{(1)}(kr_>)\left[\sum_{m=-\infty}^{\infty}e^{i2\pi m\lambda}\right]\\&=\frac{i}{4}\sum_{n=-\infty}^{\infty}e^{in(\theta-\theta_0)}J_{|n|}(kr_<)H_{|n|}^{(1)}(kr_>)\\&=(i/4)H_0^{(1)}(kR(\theta-\theta_0))\equiv K_F(\mathbf{r},\mathbf{r}_0)\,.\end{aligned}\tag{7.3a}$$

This relation illustrates the principle that a symmetric combination of the branches of a multivalued solution to a particular equation such as (2.1) returns a single-valued solution of that equation [See Ref. 7(b), pp. 266–271].

With this result in hand, let us return now to the free-space electromagnetics problem. To account for the enlarged path set, a Riemann space in which each sheet is a replica of $\mathbf{R}^2$; i.e., $P_2\equiv\mathbf{R}^2$, is introduced. The space P_∞ then resembles the spiral staircase surface associated with the logarithm function of complex analysis, and the preimages of (r,θ) are the points $(r,\theta+m2\pi)$, $m=0,\pm1,\pm2,\ldots$. The P_∞ solution $K_\infty(\mathbf{r},\mathbf{r}_0)$ remains (4.12). The folding of K_∞ onto $P^2=\mathbf{R}^2$ given by (7.3a) leads to the exact solution, the free-space propagator $K_F(\mathbf{r},\mathbf{r}_0)$. Similarly, the folding of G_∞ onto $\mathbf{R}^2=P_2$ recovers (3.6), the free-space heat conduction propagator:

$$\begin{aligned}\sum_{m=-\infty}^{\infty}&G_\infty(r,\theta+m2\pi,r_0,\theta_0;\tau)\\&=(4\pi\tau)^{-1}\exp[-(r^2+r_0^2)/4\tau]\\&\quad\times\sum_{m=-\infty}^{\infty}e^{im(\theta-\theta_0)}I_{|m|}\left(\frac{rr_0}{2\tau}\right)\equiv G_F(\mathbf{r},\mathbf{r}_0)\,.\end{aligned}\tag{7.3b}$$

This PIRS description actually provides an alternate representation of the free-space results discussed in Sec. II.

Notice that for the scattering problem where $\beta=+1$, P_+ and P_- are copies of the upper half-plane of $\mathbf{R}^2$ so that P_2 is a double covering of the upper half-plane, not $\mathbf{R}^2$ itself. Thus, even though the preimages of (r,θ) are $(r,\theta+m2\pi)$, $m=0,\pm1,\pm2,\ldots$, and the folding (7.3a) gives $K(\mathbf{r},\mathbf{r}_0)=K_F(\mathbf{r},\mathbf{r}_0)$, an image source is present on P_- and Eq. (5.6) returns the exact solution to the infinite ground plane problem, not the free-space propagator itself.

Comparing the PIRS solutions of the free-space and the wedge problems, the modification of the free-space path set by the presence of the wedge has been modeled simply by constructing the P_∞ space from replicas of the wedge P_2. This modification was responsible for reproducing the diffraction effects. In particular, it led to the evaluation of the P_∞ solution K_∞ at the resultant preimages $(r,\theta+m\Omega)$, $m=0,\pm1,\pm2,\ldots$, of (r,θ), hence,to the propagator (5.4) and the associated image term. This path set modification concept has been used in a companion paper[26] as the basis for

a path-integral derivation without discretization of the solution to the diffracting half-plane problem.

Next, the PIRS approach will be connected to several standard quantum mechanical PI methods. This discussion is facilitated by focusing attention on the related results for the heat conduction version of the wedge problem. The P_2-space propagator for the heat conduction problem corresponding to the original diffraction problem is

$$G(\mathbf{r}, \mathbf{r}_0;\tau) = \sum_{m=-\infty}^{\infty} G_\infty (r, \theta + m\Omega, r_0, \theta_0;\tau) = \sum_{m=-\infty}^{\infty} \int_{-\infty}^{\infty} e^{i\lambda(\theta-\theta_0+m\Omega)} \hat{G}_\lambda (r, r_0;\tau)\, d\lambda . \tag{7.4}$$

Clearly, it is connected to the propagator $K(\mathbf{r}, \mathbf{r}_0)$ through the relation

$$K(\mathbf{r}, \mathbf{r}_0;\tau) = \int_C e^{k^2\tau} G(\mathbf{r}, \mathbf{r}_0;\tau) d\tau .$$

Therefore, with 8.424.1 from Ref. 21, expressions equivalent to (7.4),

$$\begin{aligned} G(\mathbf{r}, \mathbf{r}_0;\tau) &= \frac{1}{\beta} \sum_{m=-\infty}^{\infty} \exp\left[i \frac{m}{\beta} (\theta - \theta_0) \right] \hat{G}_{m/\beta}(r, r_0;\tau) \\ &\equiv (4\pi\beta\tau)^{-1} \exp[-(r^2 + r_0^2)/4\tau] \\ &\quad \times \sum_{m=0}^{\infty} \epsilon_m I_{m/\beta}\left(\frac{rr_0}{2\tau}\right) \cos\left[\frac{m}{\beta}(\theta - \theta_0)\right] \end{aligned} \tag{7.5}$$

and

$$G(\mathbf{r}, \mathbf{r}_0;\tau) = (i/4\pi)(e^{-(r^2+r_0^2)/4\tau}/4\pi\tau) \times \int_A \exp\left[\frac{rr_0}{2\tau}\cos\alpha\right] \chi_\beta(\alpha, \theta - \theta_0)\, d\alpha , \tag{7.5'}$$

can be extracted from the results presented in Sec. V. They agree with those reported in Ref. 27. These representations of $G(\mathbf{r}, \mathbf{r}_0;\tau)$ accommodate several PI interpretations discussed in the literature. Of course, the expressions for the diffraction propagator will acquire similar explanations.

Notice, for instance, that (7.4) can be rewritten as

$$G(\mathbf{r}, \mathbf{r}_0;\tau) = \int_{-\infty}^{\infty} \mathcal{G}_\phi (\mathbf{r}, \mathbf{r}_0;\tau) d\phi , \tag{7.6}$$

where

$$\mathcal{G}_\phi (\mathbf{r}, \mathbf{r}_0;\tau) = \sum_{m=-\infty}^{\infty} \delta(\phi - [\theta - \theta_0 + m\Omega]) \times \mathcal{F}(\phi;\lambda)[\hat{G}_\lambda (r, r_0;\tau)] , \tag{7.7}$$

and as

$$G(\mathbf{r}, \mathbf{r}_0;\tau) = \sum_{m=-\infty}^{\infty} G_m (\mathbf{r}, \mathbf{r}_0;\tau) , \tag{7.8}$$

where

$$G_m (\mathbf{r}, \mathbf{r}_0;\tau) = \int_{-\infty}^{\infty} d\lambda \exp[i\lambda(\theta - \theta_0 + m\Omega)] \hat{G}_\lambda (r, r_0;\tau) . \tag{7.9}$$

The delta function that appears in Eq. (7.7) selects out the probability function (7.9) associated with a particular set of topologically equivalent configurations of the paths with $\phi = (\theta - \theta_0) + m\Omega$. The resultant sum (7.8) extends over all the inequivalent sets contained in the original path set. This explanation has been advocated, for example, by Inomata and Singh.[13] Another interpretation follows Schulman's point of view given, for example, in Ref. 3. The original path set in P_2 can also be decomposed into classes of homotopically equivalent paths labeled by the intersection number, $n(\gamma,\Sigma)$, of their elements γ with Σ. This intersection number is defined as follows. Let Σ_+ and Σ_- be, respectively, the wedge faces $\theta = \beta\pi$ and $\theta = 0$ so that $\Sigma = \Sigma_+ \cup \Sigma_-$. Let an intersection of a path γ with Σ_+ be positive if γ traverses Σ_+ in the direction from P_+ to P_-, negative if from P_- to P_+, and with Σ_- be positive if the crossing is from P_- to P_+, negative if its from P_+ to P_-. Also let $n_+(\gamma, C)$ and $n_-(\gamma, C)$ be the number of positive and negative crossings of C by γ. Then the intersection number of a path γ connecting $\mathbf{r}_0$ to $\mathbf{r}$ in P_2 is

$$n(\gamma, \Sigma) = [n(\gamma, \Sigma_+) + n(\gamma, \Sigma_-)]/2 \tag{7.10a}$$

where

$$n(\gamma, C) = n_+(\gamma, C) - n_-(\gamma, C) . \tag{7.10b}$$

The function G_m then represents the contribution to the propagator from those paths whose intersection number is m. These points of view are equivalent and coincide with the previous preimage description. In particular, the projection onto P_2 of a path connecting $\mathbf{r}_0$ to the preimage $\mathbf{r}_m = (r, \theta + m\Omega)$ of $\mathbf{r}$ coincides with a path γ_m whose intersection number is m. Moreover, since P_2 is isomorphic to $\mathbb{R}^2 \setminus \{0\}$, the punctured disk, γ_m is isomorphic to a path in $\mathbb{R}^2 \setminus \{0\}$ whose winding number with respect to the origin $\{0\}$ is m. Then mimicking Schulman,[3,4] the term G_m also represents the contribution to the propagator from the paths whose winding number is m.

In Refs. 13 and 14, the path integrals are evaluated directly using the homotopically equivalent path set decomposition. This is accomplished by introducing a constraint into the path integral that distinguishes inequivalent homotopy classes. This "constrained path integral" (CPI) approach realizes a path integral of the form

$$W_\lambda (\mathbf{r}, \mathbf{r}_0;\tau) = \int_\Gamma \exp[-S_\lambda (\mathbf{r}, \mathbf{r}_0;\tau)]\, \mathcal{D}\gamma , \tag{7.11}$$

where the action

$$S_\lambda (\mathbf{r}, \mathbf{r}_0;\tau) = \int_0^\tau \left(\frac{1}{4}\dot{\mathbf{r}}^2 + i\lambda\dot{\theta} \right) dt \equiv E(\lambda) + i\lambda \int_0^\tau \mathbf{A}\cdot\dot{\mathbf{r}}\, dt . \tag{7.12}$$

As noted in Refs. 12–16, the introduction of the linear term $-i\lambda \int_0^\tau \mathbf{A}\cdot\dot{\mathbf{r}}\, dt$, where $\mathbf{A} = (-y, x)/(x^2 + y^2)$, in the exponent of (7.11) facilitates the separation of the homotopy classes. The path integral (7.11) is evaluated by discretization; the desired propagator is finally generated through the expression $\int_{-\infty}^{\infty} d\phi \int_{-\infty}^{\infty} d\lambda\, e^{i\lambda\phi} W_\lambda (\mathbf{r}, \mathbf{r}_0;\tau)$. Since the linear term in (7.12) is equal to $-i\lambda \int_\gamma d\theta = -i\lambda(\theta - \theta_0)$ and since the constraint and the folding schemes are analogous (as noted above), it is recognized that the PIRS and the

CPI approaches are interrelated. Consequently, it may be possible to extend those problems (quantum mechanical and statistical problems, entangled polymer chains, potential interactions, etc.) to ones involving more general Riemann surfaces like the ones considered here, thus accommodating other physical phenomena. For instance, one obtains an interesting conclusion from the solution of the Aharonov–Bohm problem,[28] which considers quantum mechanical interference effects resulting from potentials in regions where the field is null. Path integral solutions to that problem were considered[4,13–16] from the point of view of electron paths encircling a singular point in a multiply connected space. In particular, the solution to the Aharanov–Bohm problem satisfies on $\mathbb{R}^2\backslash\{0\}$ the Schrödinger equation[28]

$$\{\partial_\tau - (i\hbar/2\mu)[\partial_r^2 + r^{-1}\partial_r + r^{-2}(\partial_\theta - i\alpha)^2]\} \times W(\mathbf{r},\mathbf{r}_0;\tau) = \delta(\mathbf{r}-\mathbf{r}_0)\delta(\tau)\,, \tag{7.13}$$

in the gauge $A_r = 0, A_\theta = \phi/2\pi r$, where ϕ is the "flux" of $\mathbf{A}$ through any circuit containing the origin (or equivalently, the flux of the corresponding magnetic field through a surface whose boundary is a circuit) and $\alpha = e\phi/2\pi\hbar c$. It can be represented as

$$W(\mathbf{r},\mathbf{r}_0;\tau) = \sum_{m=-\infty}^{\infty}\int_{-\infty}^{\infty} d\lambda \exp[i(\lambda+\alpha)(\theta-\theta_0+2\pi m)] \times \hat{G}_\lambda(r,r_0;i\hbar\tau/2\mu) = \sum_{m=-\infty}^{\infty} W_n(\mathbf{r},\mathbf{r}_0;\tau)\,, \tag{7.14}$$

which is a variant of the CPI expressions derived in Refs. 13–15. The corresponding P_2-space problem has the solution

$$\tilde{W}(\mathbf{r},\mathbf{r}_0;\tau) = \sum_{m=-\infty}^{\infty}\int_{-\infty}^{\infty} d\lambda \exp[i(\lambda+\alpha)(\theta-\theta_0+m\Omega)] \times \hat{G}_\lambda(r,r_0;i\hbar\tau/2\mu)\,. \tag{7.15}$$

Interference between the partial propagators W_m and W_n $(m\neq n)$ of (7.14) produces observable interference patterns that depend upon the encircled flux *and* the topological winding number.[15,29,30] On the other hand, quantization of the flux ϕ encircled by the paths can be inferred from the total propagator (7.14) by applying the (two-dimensional) arguments given in Ref. 13. Letting the singular point represent a magnetic monopole with flux $\phi = 4\pi g$ and setting $\mathbf{r} = \mathbf{r}'$, self-consistency requires $2\pi\alpha = \text{integer}\times 2\pi = 2\pi n$ so that the quantization condition derived by Dirac,[31] $g = n(\hbar c/2e)$, is recovered. Similar arguments applied to (7.15) yield $\alpha\Omega = 2\pi n$ or $g = (n/\beta)(\hbar c/2e)$, which means the wedgelike solution corresponds to fractional charge quantization. This result is extended to more general fractions simply by incorporating Riemann surfaces with more sheets. For instance, a Riemann surface P_3 constructed from three copies of P would make $\Omega = 3(\beta\pi)$ and then a choice of $\beta = 2$ would give $g = (n/3)$ (57.5e). Thus, the PIRS approach may have some applications in the analysis of quantum field problems involving fractionally charged particles such as quarks.

The special case of the half-plane problem $(\beta = 2)$ leads to another very interesting characteristics of the P_2-space heat conduction and wedge propagators. These half-plane propagators, denoted explicitly by G_2 and K_2, have the forms

$$G_2(\mathbf{r},\mathbf{r}_0;\tau) = (8\pi\tau)^{-1}\exp[-(r^2+r_0^2)/4\tau] \times \sum_{m=0}^{\infty}\epsilon_m I_{m/2}(rr_0/2\tau)\cos\left[m\left(\frac{\theta-\theta_0}{2}\right)\right], \tag{7.16}$$

$$K_2(\mathbf{r},\mathbf{r}_0) = \frac{i}{8}\sum_{m=0}^{\infty}\epsilon_m J_{m/2}(kr_>)H_{m/2}^{(1)}(kr_>) \times\cos[m((\theta-\theta_0)/2)]\,. \tag{7.17}$$

For example, with (4.9), (3.6), and the relations 8.406.1, 8.476.4, and 8.511.4 of Ref. 21,

$$\exp(x\cos\phi) = \sum_{m=0}^{\infty}\epsilon_m I_m(x)\cos(m\phi)\,, \tag{7.18}$$

the expression (7.16) yields the relation

$$\begin{aligned} &G_2(r,\theta+2\pi,r_0,\theta_0;\tau) \\ &= \frac{1}{2}\sum_{m=0}^{\infty}\epsilon_m\hat{G}_{m/2}(r,r_0;\tau)\cos\left[m\left(\frac{\theta-\theta_0}{2}\right)+m\pi\right] \\ &= \frac{1}{2}\sum_{\text{even }m}\hat{G}_{m/2}(r,r_0;\tau)\cos\left[m\left(\frac{\theta-\theta_0}{2}\right)\right] \\ &\quad - \frac{1}{2}\sum_{\text{odd }m}\hat{G}_{m/2}(r,r_0;\tau)\cos\left[m\left(\frac{\theta-\theta_0}{2}\right)\right] \\ &= \sum_{m=0}^{\infty}\hat{G}_m(r,r_0;\tau)\cos[m(\theta-\theta_0)] - G_2(r,\theta,r_0,\theta_0;\tau) \\ &= G_F(\mathbf{r},\mathbf{r}_0;\tau) - G_2(r,\theta,r_0,\theta_0;\tau) \end{aligned}$$

or

$$G_2(r,\theta+2\pi,\mathbf{r}_0;\tau) = -G_2(r,\theta,\mathbf{r}_0;\tau) + G_F(\mathbf{r},\mathbf{r}_0;\tau)\,. \tag{7.19}$$

This also means

$$G_2(r,\theta+4\pi,r_0,\theta_0;\tau) = G_2(r,\theta,r_0,\theta_0;\tau)\,. \tag{7.20}$$

Similarly, the half-plane propagator satisfies

$$K_2(r,\theta+2\pi;\mathbf{r}_0) = -K_2(r,\theta;\mathbf{r}_0) + K_F(\mathbf{r},\mathbf{r}_0)\,, \tag{7.21}$$

$$K_2(r,\theta+4\pi;\mathbf{r}_0) = K_2(r,\theta;\mathbf{r}_0)\,. \tag{7.22}$$

Treating $G_2(r,\theta,2\pi;\mathbf{r}_0)$ and $G_2(r,\theta;\mathbf{r}_0)$ as the values of different branches of G_2 at corresponding points, Eq. (7.19) demonstrates that the half-plane propagator itself exhibits the multivalued solution property:

$$G_2(r,\theta;\mathbf{r}_0) + G_2(r,\theta+2\pi;\mathbf{r}_0) = G_F(\mathbf{r},\mathbf{r}_0)\,. \tag{7.19'}$$

In the half-plane problem Σ is actually a branch line, Σ_+ being its "bottom side" and Σ_- its "top side." Equation (7.20) expresses the continuity of G_2 during the transition through Σ_- from P_- to P_+. On the other hand, evaluating (7.19) at $\theta = \epsilon$, $0<\epsilon\ll 1$, one obtains the transition condition

$$G_2(r,2\pi+\epsilon;\mathbf{r}_0) = -G_2(r,\epsilon;\mathbf{r}_0) + G_F(\mathbf{r},\mathbf{r}_0)\,, \tag{7.23}$$

for the values of G_2 on opposite sides of the branch line Σ, the point (r,ϵ) being in P_+ near Σ_- and $(r,2\pi+\epsilon)$ being in P_-

near Σ_+. Equation (7.23) is also recognized as the transition condition for a Riemann–Hilbert problem[11] for G_2. The -1 coefficient of the transition condition indicates a square root behavior of G_2 near the edge of the half-plane. The corresponding diffraction propagator $K_2(\mathbf{r},\mathbf{r}_0)$ clearly also shares these properties. They are discussed in detail in Ref. 26. Notice, in particular, that requiring K_2 to be bounded at $r=0$ and interpreting the K_2 version of (7.23) as a Riemann–Hilbert problem leads one to Meixner's edge condition[32]

$$\lim_{r\to 0} K_2(\mathbf{r},\mathbf{r}_0) \sim \mathcal{O}(r^{1/2}) .$$

This square root behavior also reinforces the choice of the two-sheeted P_2-space for our analysis.

Similarly, consider the value of G_2 as $\mathbf{r}$ traverses a closed path in the original problem space, where $(r,\theta) = (r,\theta \bmod 2\pi)$, that encloses the edge. If the path has an even winding number, Eq. (7.20) implies that the values of G_2 at the coincident end points of the path are identical, hence that G_2 returns to its original value along a double loop. On the other hand, if its winding number is odd, Eq. (7.19) returns different end-point values. The propagator G_2 does not return to its original value along a single loop but to its negative modified by G_F. Thus, the monodromy group associated with the half-plane problem is $\{1, e^{i\pi} = -1\}$, which is also characteristic of the square root behavior and again indicates the desirability of the two-sheeted P_2-space.

Analogous solution characteristics were utilized by Kadonoff and Kohmoto in their treatment[33] of the two-component spinor correlation function. There, the SMJ (Sato, Miwa, and Jimbo) analysis of the two-dimensional Ising model in terms of the solutions to a two-dimensional version of the Dirac equation and extensions of their analysis were discussed. Since the two-dimensional Dirac and Maxwell equations havae similar forms, the PIRS approach should have applications in statistical mechanics problems as well.

In addition, because potential and heat equation problems are interrelated (probabilistic potential theory[34]), potential problems and the techniques that have been developed to solve them may also prove to be very useful for analyzing the corresponding scattering problems. This concept was first noted by MacDonald.[35] In particular, a P_∞-type analysis of the wedge-potential problem given by Davis and Reitz[36] leads to a solution that is readily connected to the corresponding wedge diffraction solution. Let

$$\Lambda_{\pm}(\alpha,\psi) = (1/2\pi i)(1/(\psi \pm \alpha)),$$

so that

$$\Lambda(\alpha,\psi) = \Lambda_+(\alpha,\psi) - \Lambda_-(\alpha,\psi),$$

and let $\mathcal{G}_F[R(\theta-\theta_0)]$ be the free-space Green's function for a particular equation (Helmholtz, heat conduction, and Laplace operators in two or three dimensions). The P_∞-space propagator in any of the corresponding (straight) wedge problems can then be represented in the form

$$K_\infty(\mathbf{r},\mathbf{r}_0) = \int_A \mathcal{G}_F[R(\theta-\theta_0)]\Lambda(\alpha,\theta-\theta_0)d\alpha ; \tag{7.24}$$

hence, the associated P_2-space result is

$$K(\mathbf{r},\mathbf{r}_0) = \sum_{m=-\infty}^{\infty} \int_A \mathcal{G}_A[R(\theta-\theta_0)]\Lambda(\alpha,\theta-\theta_0+m\Omega)d\alpha$$
$$= \frac{i}{4\pi}\int_A \mathcal{G}_F[R(\theta-\theta_0)]\chi_\beta(\alpha,\theta-\theta_0)d\alpha . \tag{7.25}$$

On the other hand, numerical solutions to general potential problems have been constructed based upon path-integral concepts. Generalizations of these schemes to the PIRS point of view would allow solution, for instance, of the curved diffracting wedge problem (see Ref. 37, for example). A coordinate net could be constructed in a P_2-space corresponding to the exterior of the wedge, and the paths and their contributions to the path integral could then be computed numerically in a manner similar to the general potential problem approach. Such a numerical scheme would greatly extend the applicability of the PIRS technique.

Finally, Schulman[38] has remarked that the use of the Riemann surface in connection with path integrals is "an embarrassment to purists." On the contrary, as demonstrated in this paper, the PIRS approach is natural and essential for problems in which boundary surfaces or constraints are present. The RS removes the boundaries or constraints thus allowing the PI to be calculated over a path set having no special restrictions. The RS can then be viewed as containing the PI's original path set information, hence, as arising from a purely path integral context.

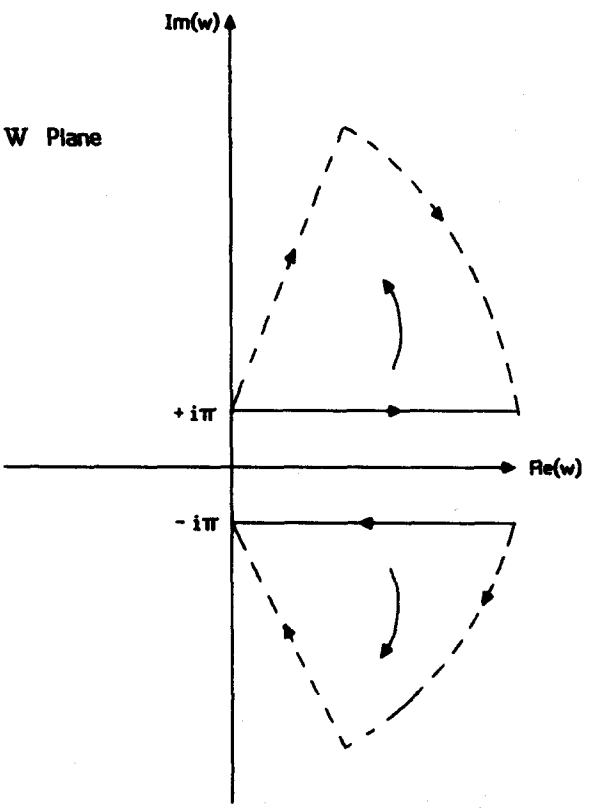

FIG. 4. Deformation of the modified Bessel's function contour.

ACKNOWLEDGMENTS

The author would like to express his deepest appreciation to his former advisor, Professor G. A. Deschamps, for his invaluable comments and suggestions as this paper evolved.

This work was supported in part by National Science Foundation Grant No. NSF-ENG-77-20820 and by the Lawrence Livermore National Laboratory under the auspices of the U. S. Department of Energy under Contract No. W-7405-ENG-48.

APPENDIX: DERIVATION OF THE RADIAL PORTION OF THE P_∞ PROPAGATOR

To generate Eq. (4.9) from Eq. (4.8), first consider the integrations over the angle variables. A typical one has the form

$$f_\lambda(x) = \int_{-\infty}^{\infty} dy \exp(x\cos y - i\lambda y), \tag{A1}$$

where x and λ are real numbers. On the other hand, the modified Bessel's function is given by 6.22.3 in Ref. 39 as

$$I_\lambda(x) = \frac{1}{2\pi i}\int_{\infty - i\pi}^{\infty + i\pi} dw \exp[x\cosh w - \lambda w]. \tag{A2}$$

As shown in Fig. 4, the contour of integration is taken to be $-i\pi + \infty \to -i\pi \to i\pi \to i\pi + \infty$.

Assuming that λ and x are non-negative, the contours parallel to the real axis can be deformed to the ones shown in Fig. 4. The contribution from the arcs at infinity are zero leaving only an integral along the imaginary axis. A change of variables then gives $f_\lambda(x) = 2\pi I_\lambda(x)$. Thus, Eq. (4.8) becomes

$$\hat{G}_\lambda(r,r_0;\tau) = \lim_{N\to\infty}\frac{1}{2\pi}(2\epsilon)^{-N}\int_0^\infty\cdots\int\exp\left[-\sum_{j=1}^{N}\frac{r_j^2+r_{j-1}^2}{4\epsilon}\right] I_{|\lambda|}\left(\frac{r_1 r_0}{2\epsilon}\right)\cdots I_{|\lambda|}\left(\frac{r_N r_{N-1}}{2\epsilon}\right)\prod_{j=1}^{N-1} r_j\, dr_j. \tag{A3}$$

The non-negativity of the order of the modified Bessel's function has been assured by restricting λ to its absolute value.

Since for $Re(\eta) > -1$ and $Re(\xi) > 0$ (see Ref. 21, 6.633.4),

$$\int_0^\infty \exp(-\xi x^2) I_\eta(ax) I_\eta(bx) x\, dx = \frac{1}{2\xi}\exp\left(\frac{a^2+b^2}{4\xi}\right) I_\eta\left(\frac{ab}{2\xi}\right), \tag{A4}$$

it is readily shown that the jth integration in (A3) yields

$$\begin{aligned}
&\frac{\alpha^{j-1}}{j}\exp\left[\frac{-r_0^2}{j(2\alpha)}\right]\int_0^\infty \exp\left[-\left(\frac{j+1}{j}\right)\frac{r_j^2}{(2\alpha)}\right] I_{|\lambda|}\left(\frac{r_{j+1}r_j}{\alpha}\right) I_{|\lambda|}\left(\frac{r_j r_0}{j\alpha}\right) r_j\, dr_j \\
&= \frac{\alpha^{j-1}}{j}\left(\frac{j\alpha}{j+1}\right)\exp\left[\frac{-r_0^2}{j(2\alpha)} + \frac{r_0^2}{j(j+1)(2\alpha)} + \left(\frac{j}{j+1}\right)\frac{r_{j+1}^2}{(2\alpha)}\right] I_{|\lambda|}\left[\frac{r_0}{j\alpha}\cdot\frac{r_{j+1}}{\alpha}\cdot\frac{j\alpha}{(j+1)}\right] \\
&= \frac{\alpha^j}{j+1}\exp\left[\frac{-r_0^2}{(j+1)(2\alpha)}\right]\exp\left[\left(\frac{j}{j+1}\,\frac{r_{j+1}^2}{(2\alpha)}\right)\right] I_{|\lambda|}\left[\frac{r_{j+1}r_0}{(j+1)\alpha}\right],
\end{aligned} \tag{A5}$$

where $\alpha = 2\epsilon$. Therefore, because $N\alpha = 2N\epsilon \equiv 2\tau$, Eq. (A3) becomes

$$\begin{aligned}
\hat{G}_\lambda(r,r_0;\tau) &= \lim_{N\to\infty}\frac{1}{2\pi}\alpha^{-N}\exp\left(\frac{-r^2}{2\alpha}\right)\left\{\frac{\alpha^{N-1}}{N}\exp\left(\frac{-r_0^2}{2N\alpha}\right)\exp\left[\frac{(N-1)r_N^2}{2N\alpha}\right] I_{|\lambda|}\left(\frac{r_N r_0}{N\alpha}\right)\right\} \\
&= \lim_{N\to\infty}\frac{1}{2\pi N\alpha}\exp\left[\frac{-(r^2+r_0^2)}{2N\alpha}\right] I_{|\lambda|}\left(\frac{rr_0}{N\alpha}\right) = (4\pi\tau)^{-1}\exp\left(\frac{-(r^2+r_0^2)}{4\tau}\right) I_{|\lambda|}\left(\frac{rr_0}{2\tau}\right).
\end{aligned} \tag{A6}$$

A physical explanation of the restriction that λ be non-negative is now apparent. It corresponds precisely to the physical property that the propagator (A6) be finite as $r\to 0$; i.e., $I_{-\lambda}$ is proportional to K_λ, which becomes infinite as its argument nears zero. Note that a generalization of this procedure was developed in Ref. 40 and was used in a similar fashion in 13.

[1] J. S. Dowker, J. Phys. A: Gen. Phys. **5**, 936 (1972).
[2] M. G. G. Laidlaw and C. Morette-DeWitt, Phys. Rev. D **3**, 1375 (1971).
[3] L. Schulman, Phys. Rev. **176**, 1558 (1968).
[4] L. Schulman, J. Math Phys. **12**, 304 (1971).
[5] L. Schulman, *Functional Integration and Its Applications* (Claredon, Oxford, 1975), Chap. 12.
[6] V. S. Buslaev, in *Topics in Mathematical Physics*, edited by Sh. Berman (Consultants Bureau, New York, 1967) (English translation), p. 67.
[7] A. Sommerfeld, (a) Math. Ann. **47**, 317 (1896); (b) *Optics* (Academic, New York, 1954), Sec. 38.
[8] H. S. Carslaw, Proc. London Math. Soc. Ser. 2 **30**, 121 (1899).
[9] S. W. Lee, J. Math. Phys. **19**, 1414 (1978).
[10] J. B. Keller, J. Opt. Soc. Am. **52**, 116 (1962).
[11] F. D. Gakhov, *Boundary Value Problems* (Pergamon, New York, 1966); E. I. Zverovich, Russian Math. Surveys **26**, 117 (1971); R. W. Ziolkowski, SIAM J. Math. Anal. **16**, 358 (1985).
[12] S. F. Edwards, Proc. Phys. Soc. London **91**, 513 (1967).
[13] A. Inomata and V. A. Singh, J. Math. Phys. **19**, 2318 (1978).
[14] C. C. Gerry and V. A. Singh, Phys. Rev. D **20**, 2550 (1979).
[15] C. C. Bernido and A. Inomata, Phys. Lett. A **77**, 394 (1980); J. Math. Phys. **22**, 715 (1981).
[16] F. W. Wiegel, Physica A **109**, 609 (1981).
[17] G. A. Deschamps, "Wedge diffraction," paper presented at the USNC/

URSI-IEEE Meeting, Boulder, Colorado, January, 1975.
[18]L. B. Felsen and N. Marcuvitz, *Radiation and Scattering of Waves* (Prentice–Hall, Englewood Cliffs, NJ, 1973).
[19]M. Kac, Trans. Am. Math. Soc. **65**, 1 (1949).
[20]S. F. Edwards and Y. V. Gulyaev, Proc. R. Soc. London Ser. A **279**, 229 (1964).
[21]I. S. Gradshteyn and I. M. Ryzhik, *Table of Integrals, Series, and Products* (Academic, New York, 1965).
[22]I. Stakgold, *Boundary Value Problems of Mathematical Physics* (Macmillan, New York, 1967), Vol. I.
[23]H. S. Carslaw, Proc. London Math. Soc. Ser. 2 **18**, 291 (1919).
[24]*Electromagnetic and Acoustic Scattering by Simple Shapes*, edited by J. J. Bowman, T. B. A. Senior, and P. L. E. Uslenghi (North-Holland, Amsterdam, 1969), Chap. 6.
[25]T. T. Wu, Phys. Rev. **104**, 1201 (1956).
[26]R. W. Ziolkowski, UCRL-91607, Lawrence Livermore National Laboratory, 1984.
[27]H. S. Carslaw, Proc. London Math. Soc. Ser. 2 **8**, 365 (1910).
[28]Y. Aharanov and D. Bohm, Phys. Rev. **115**, 485 (1959).
[29]A. Inomata, Phys. Lett. A **95**, 176 (1983).
[30]B. S. Deaver and G. B. Donaldson, Phys. Lett. A **89**, 178 (1982); A. Tonomura, T. Matsuda, R. Suzuki, A. Fukuhara, N. Osakabe, H. Umezaki, J. Endo, K. Shinagawa, Y. Sugita, and H. Fujiwara, Phys. Rev. Lett. **48**, 1443 (1982).
[31]P. A. M. Dirac, Proc. R. Soc. London Ser. A **133**, 60 (1931); Phys. Rev. **74**, 817 (1949).
[32]D. S. Jones, *The Theory of Electromagnetism* (Macmillian, New York, 1964), pp. 566–569.
[33]L. P. Kadanoff and M. Kohmoto, Ann. Phys. **126**, 371 (1980).
[34]R. Hersh and R. J. Griego, Sci. Am. **220** (3), 66 (1969).
[35]H. M. MacDonald, Proc. London Math. Soc. Ser. 2 **14**, 410 (1915).
[36]L. C. Davis and J. R. Reitz, J. Math. Phys. **16**, 1219 (1975).
[37]S. W. Lee and G. A. Deschamps, IEEE Trans. Antennas Propag. **AP-24**, 25 (1976).
[38]L. S. Schulman, *Techniques and Approaches of Path Integration* (Wiley, 1981), pp. 40 and 41.
[39]G. N. Watson, *Theory of Bessel Functions* (Cambridge U. P., London, 1966), 2nd ed.
[40]D. Peak and A. Inomata, J. Math. Phys. **10**, 1422 (1969).